Proceedings of

SHIRMS 2008

1st Southern Hemisphere International Rock Mechanics Symposium

16–19 September 2008, Perth, Western Australia

Volume One
Mining and Civil

EDITORS

Yves Potvin
Australian Centre for Geomechanics, Australia

John Carter
The University of Newcastle, Australia

Arcady Dyskin
The University of Western Australia, Australia

Rob Jeffrey
CSIRO Petroleum, Australia

ISRM Regional Symposium

ISRM

ACG AUSTRALIAN CENTRE FOR GEOMECHANICS

CSIRO | Curtin University | University of WA
Joint Venture

SHIRMS 2008 – Y. Potvin, J. Carter, A. Dyskin, R. Jeffrey (eds)
 ISBN 978-0-9804185-5-2

Numerical Simulation of a Multi-Reef Tabular Mining Layout in a South African Platinum Mine

J.A.L. Napier *CSIR Pretoria and the University of the Witwatersrand, South Africa*

D.F. Malan *Groundwork Consulting (Pty) Ltd, South Africa*

Abstract

Some of the key problems facing rock engineers on mines in the Bushveld Complex are the design of stable panel spans, optimum pillar dimensions and assessing hangingwall stability. A particularly difficult problem is encountered in some mines where multi-reef tabular layouts are exploited with a small middling between the reefs. As exploitation of the lower UG2 reef was never envisioned in the early years of platinum mining, the layout of the upper Merensky reef was never optimised for multi-reef extraction. This makes the design of UG2 layouts very problematic. To assist with these designs, the newly developed TEXAN computer code has been found to be very useful. The paper gives a brief overview of the code and then describes a case study of the stress analysis of a multi-reef tabular mining layout.

1 Introduction

Platinum mining in the Bushveld Complex in South Africa has gained much prominence in recent years. This production is set to increase further as the eastern limb of the Bushveld Complex is currently undergoing a significant expansion programe. Two reefs are currently of economic importance namely the upper Merensky reef (a pegmatiodal pyroxenite) and the lower UG2 reef (a chromitite layer). Both reefs are tabular in nature with a small dip (9 to 18°). The stoping width on both reefs typically varies from 1.1 to 1.5 m. Based on the economic importance of these mining activities to South Africa, it is vital that engineers are provided with the most appropriate tools to ensure the optimum design of mine layouts and cost-effective support systems. Two of the key problems facing rock engineers on mines in the Bushveld Complex are the design of stable panel spans (Watson and Noble, 1997; Watson and Roberts, 1999), optimum pillar dimensions (Ryder et al., 1997) and assessing hangingwall stability (Akermann et al., 2003). Historically, panel spans and pillar dimensions were designed largely through trial and error and knowledge of designs that were successful in the past. Greater attention has recently been given to the use of numerical modelling (Day and Godden, 2000; Joughin et al., 2000; Roberts et al., 2002), various rock mass rating systems (Hartman, 2000) and pillar design methodologies (Wesseloo and Swart, 2000; Ryder and Jager, 2002) to assist in this process. A particularly difficult problem is encountered in some mines where the middling between the Merensky and UG2 reefs is very small. In some areas this can be as small as 18 m. As exploitation of the lower UG2 reef was only made possible by advances in metallurgical processes in the 1970s, the layout of the upper Merensky reef was never optimised for multi-reef extraction. This makes the design of UG2 layouts very difficult. A new displacement discontinuity boundary element program, TEXAN, has been developed (Napier and Malan, 2007) to facilitate the analysis of shallow layout problems which include a large number of small pillars. This paper gives a brief overview of the code and then describes a multi-reef tabular mining layout case study.

2 Overview of the TEXAN code

Historically, the decade from 1960 to 1970 was particularly important in the development of the field of rock engineering in South Africa. Of particular significance were studies (Ortlepp and Nicoll, 1965) showing that the far field rock mass behaviour in deep hard rock mines can be determined accurately by assuming an elastic rock mass and by assuming that tabular excavations can be approximated to be open cracks having the same plan-shape as the excavation (Salamon, 1964). The approach has subsequently been dubbed the displacement discontinuity boundary element method (DDM). Initial applications of the DDM were directed mainly to the design of gold mine stabilising pillars and to the assessment of backfill layout placement

policies for the reduction of rockburst risks. In these cases, it is generally adequate to utilise so-called "infinite" depth displacement discontinuity influence functions. This assumption becomes inadequate in the analysis of shallow-depth platinum mining problems. In addition, it is often important in these cases to assess tensile stress distributions near excavation surfaces. The TEXAN program addresses these shortcomings by including fully analytic half-space influence functions and by allowing higher order element displacement discontinuity shape functions. In addition, element shapes may be assigned as triangles or quadrilaterals to facilitate the representation of irregular pillar layout geometries. Considerable attention has also been given to implement an accurate multi-level solution scheme to enable the efficient solution of large-scale problems. A further feature of the program is to allow special two-dimensional (2D) plane strain sub-analyses (including anti-plane strains) within the three-dimensional (3D) problem background. The technical details of the TEXAN program are described in Napier and Malan (2007).

3 Underground observations and measurements in a UG2 stope

A particular mining layout was studied at a platinum mine as anomalously high roof to floor deformations were observed in one of the panels. The layout is shown in Figure 1. The upper Merensky reef was partially extracted and mining commenced on the lower UG2 reef horizon. As the middling is only 18 m thick in this area, stability problems are typically encountered when the UG2 panels are being mined below the Merensky remnants. To monitor the stability of these panels, closure instrumentation was installed in Panels 4N, 5N and 6N on the UG2 reef (Figure 1).

In this paper closure refers to the relative movement of the hangingwall and footwall normal to the plane of the excavation and includes both elastic and inelastic deformations. The elastic component of closure is referred to as convergence. Ride refers to the relative movement of the hangingwall and footwall parallel to the plane of the excavation.

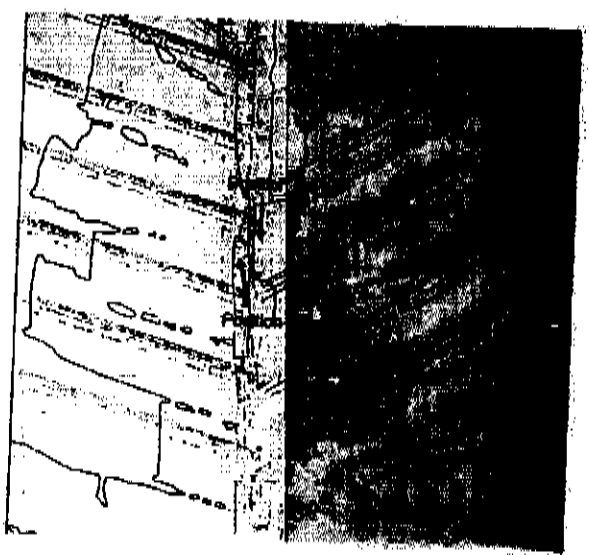

Figure 1 Mining layout in the area of interest. The positions indicated on the figure indicate where the photographs (Figures 2, 3 and 4) were taken

Visual observations indicated that high rates of closure were experienced in Panel 4N. Of some concern was the significant strike ride component observed in Panel 4N (Figures 2 and 3), as this was not previously seen in other areas where Merensky remnants were being undermined. A fall of ground was also observed next to the abutment in Position B (Figure 4).

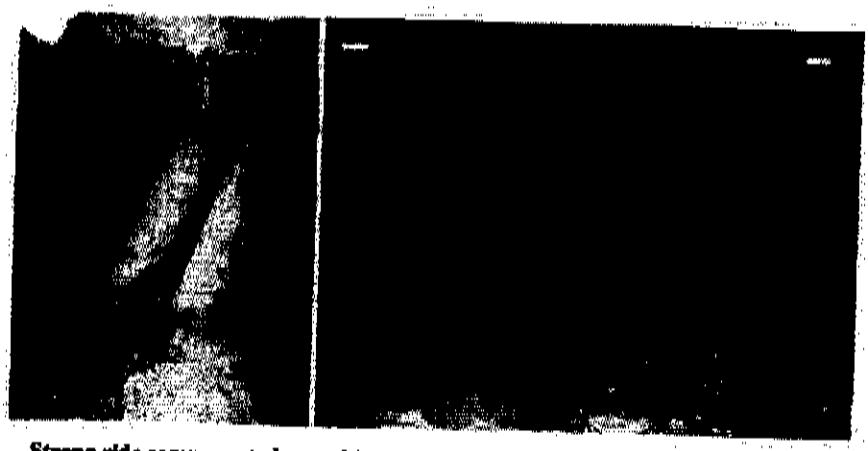

Figure 2 Strong ride component observed in the back area of Panel 4N close to the centre gully (Position A, Figure 1). The sense of the ride component is such that the hangingwall moved towards the centre gully

Figure 3 Fall of ground in the ledge of Panel 4S (Position B, Figure 8). Observations indicate that this fall appears to have been caused by shear failure in the hangingwall next to the abutment on this ledge

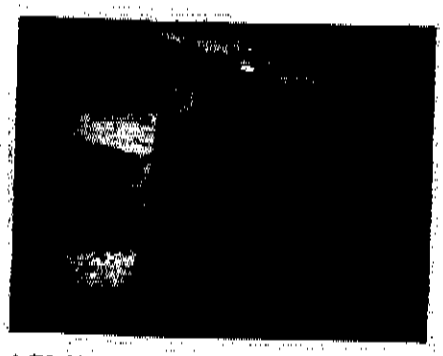

Figure 4 Conditions in Panel 6N. Significantly less closure and ride was observed in this panel as it was being mined in overstoped ground

3.1 Closure and ride measurements

A number of closure-ride stations were installed in Panels 4N, 5N and 6N. The stations consist of three anchors in the hangingwall and an anchor in the footwall. From successive measurements between the three pegs in the hangingwall and the peg in the footwall, the closure as well as the strike and dip ride components can be computed. The closure and ride graphs for Panel 4N (below the remnant in high stress conditions) and Panel 6N (in overstoped ground and therefore destressed) are given in Figures 5 to 8. Note the high rates of closure below the remnant (5.6 mm/day) compared to the low rates (0.41 mm/day) in the overstoped ground. A strike ride component of 30 mm was recorded below the remnant over a two week monitoring period, while it was very small in the panel below the overstoped ground.

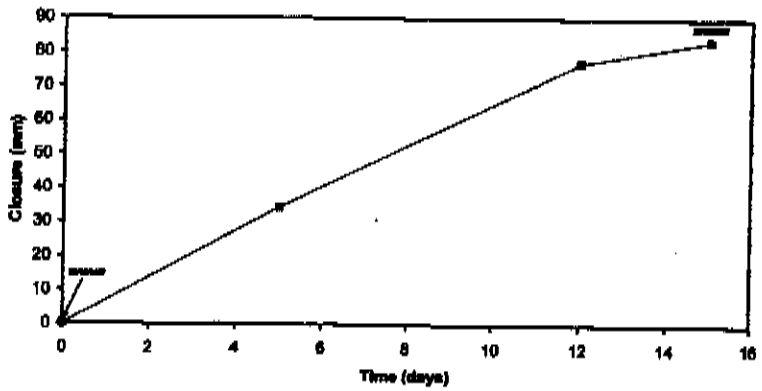

Figure 5 **Closure as a function of time measured in panel 4N. The average rate of closure was 5.6 mm/day**

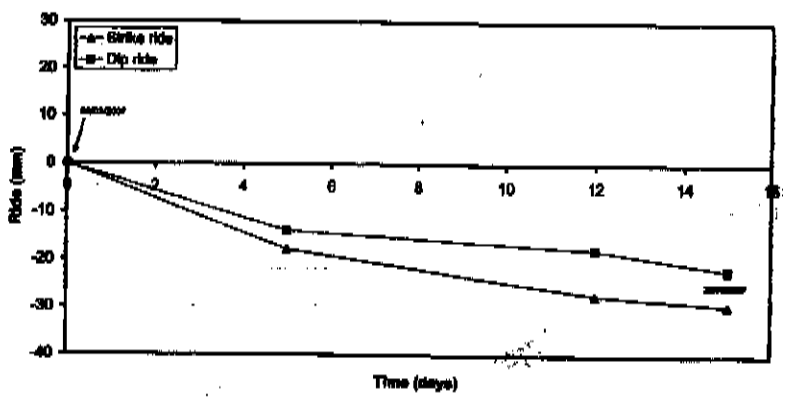

Figure 6 **Ride as a function of time measured in Panel 4N. The following sign convention is used for the ride graphs: A negative strike ride implies that the footwall peg moved in the direction of the advancing face relative to the hangingwall pegs. A negative dip ride implies that the footwall peg is moving up-dip relative to the hangingwall pegs. Note the high strike ride component of more than 30 mm in a two week period. The sense of ride agrees with the underground observations where the top of the packs leaned over towards the centre gully**

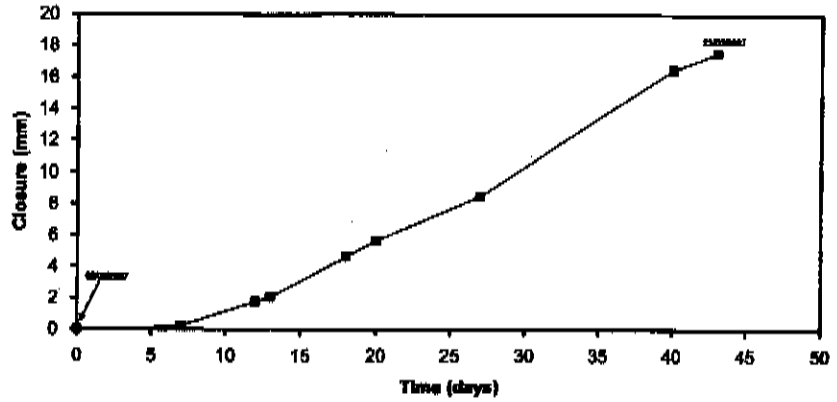

Figure 7 **Closure as a function of time measured in Panel 6N. The average rate of closure was 0.41 mm/day**

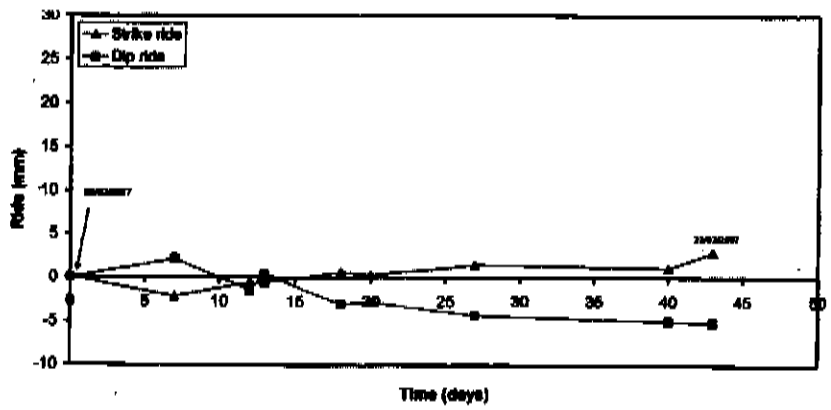

Figure 8 **Ride as a function of time measured in Panel 6N. The same sign convention as described in Figure 6 is used. Note that the strike ride is significantly less than that recorded in Panel 4N**

4 Numerical modelling

4.1 Mining geometry and modelling parameters

The modelling parameters used are given in Table 1. In this table, the k-ratio denotes the ratio of the horizontal to vertical field stress components.

Table 1 **Parameters used in the numerical models**

Parameter	Value
Young's Modulus	68 GPa
Poisson's ratio	0.28
k-ratio	1
Average overburden density	3200 kg/m^3

The layout chosen for detailed investigation is shown in Figure 9 and covers an area of 803 x 807 m. This area of interest was discretised using triangular elements as shown in Figures 10 and 11.

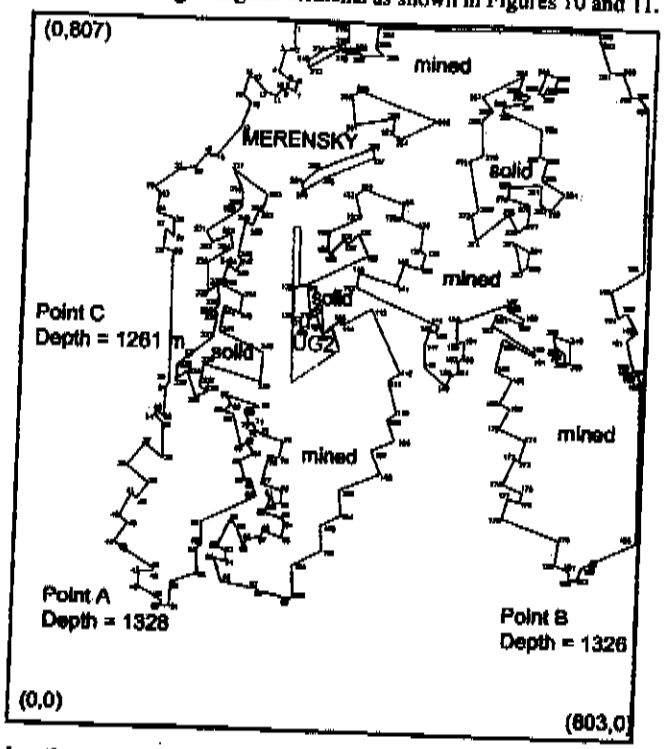

Figure 9 Approximation of the stopes and remnants by polygons to assist with the digitising process

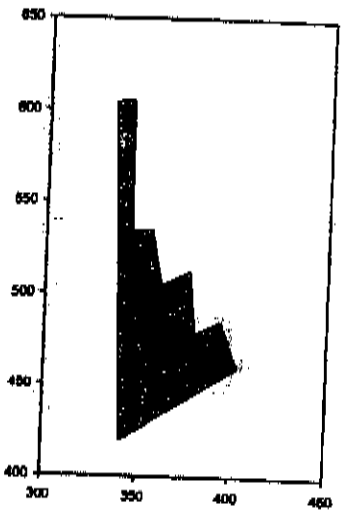

Figure 10 Discretisation used for the UG2 reef

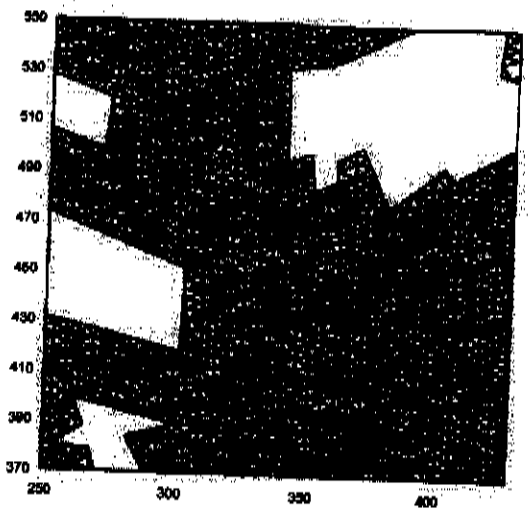

Figure 11 Part of the Merensky reef showing the discretisation used

4.2 Modelling results

Figure 12 illustrates the superimposed Merensky and UG2 mining outlines. In the first simulated mining step, the UG2 was left unmined to examine the stress acting on this reef plane as a result of the overlying Merensky remnant configuration. The resulting stress component values normal to the UG2 reef plane are shown in Figure 13. It is apparent that the stress below the Merensky remnant (line A-B, Figure 12) is very high compared to the over-mined areas (line E-F, Figure 12). The virgin vertical stress is approximately 40 MPa at this depth.

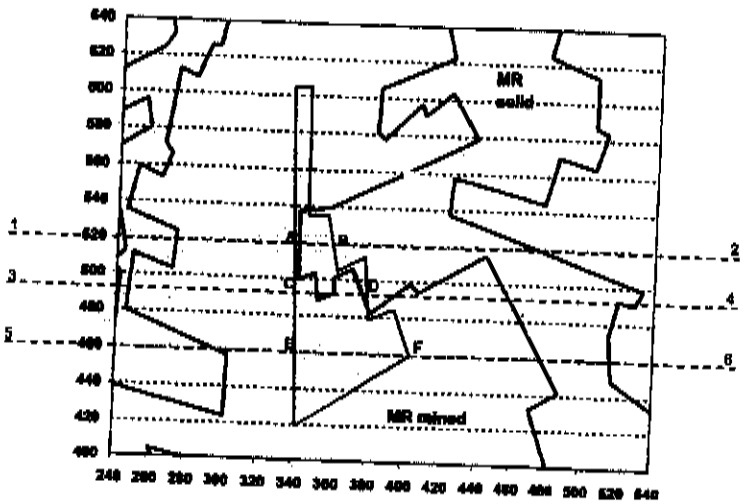

Figure 12 Superimposed Merensky and UG2 mining outlines

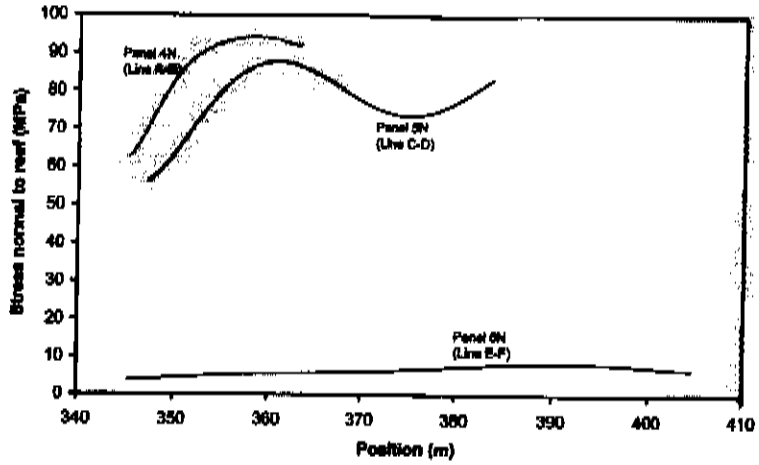

Figure 13 Simulated stress normal to the UG2 reef plane prior to any mining occurring on this reef horizon. The lines in the annotations refer to the lines in Figure 12. The peak stress in Panel 4N (94 MPa) is more than twice the virgin vertical stress at this depth

The simulated convergence and strike ride components when mining the UG2 panels are given in Figures 14 and 15. Note the significant strike ride components in Panels 4N and 5N. The sense of ride is also similar to that observed underground. A direct comparison with the actual measurements in Figures 5 to 8 was not attempted as an isotropic elastic constitutive model was assumed for the numerical models, whereas the underground behaviour is dominated by large inelastic movements. Significant time-dependent closure components are also observed underground (Malan et al., 2007). The objective of the modelling was to gain some insights into the mechanism of failure observed underground and not to replicate the magnitude of the underground displacements. The mechanism of failure is further explored in Section 4.3. The curves in Figures 14 and 15 illustrates the total convergence when simulating the entire mining area whereas the actual measurements only show the increase in closure for a few mining increments. Note that in Panel 4N (Figure 5), the increase in closure for a few mining increments is more than the total simulated elastic convergence (Figure 14), highlighting the significance of the inelastic displacements.

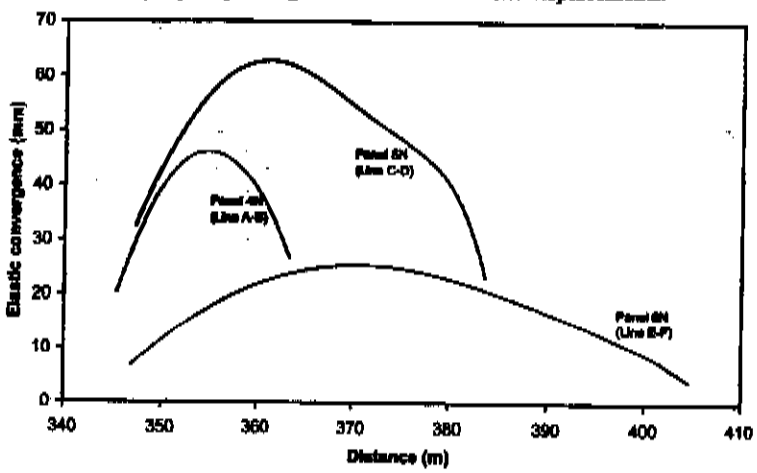

Figure 14 Simulated elastic convergence in the UG2 panels. The specific annotations refer to the lines in Figure 12

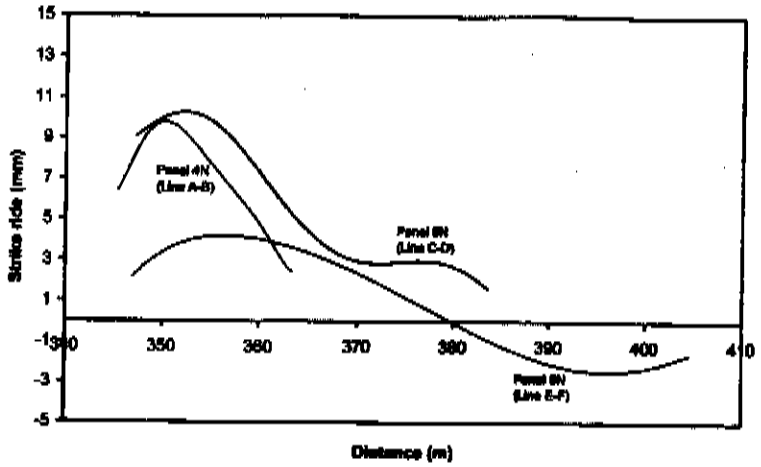

Figure 15 Simulated strike ride in the UG2 panels. The annotations in each curve refer to the lines in Figure 12. The convention used in the code implies that for a positive strike ride, the UG2 hangingwall in Figure 12 moves towards the left relative to the footwall. The simulated sense of ride is therefore similar to that measured underground where the support leans back towards the centre gully (Figure 2)

4.3 Deformation mechanism

A comparison between the simulated elastic movements and underground closure measurements illustrated that significant inelastic movements occurred in the underground panels. This was confirmed by the recording of the closure in a continuous fashion, which indicated a significant time-dependent closure component (Malan et al., 2007). Further simulations were therefore conducted to investigate a possible mechanism that contributed to the large closure and ride components for the layout in Figure 9.

The TEXAN code can be used to compute the displacement vectors at off-reef locations and convert these into a distorted mesh plot to assist with an interpretation of the near reef deformation modes. These distorted mesh plots were computed on benchmark sheets normal to the reef planes to illustrate the deformation of the middling between the UG2 and Merensky reefs. A distortion factor of 200 was used in these plots to highlight the relative displacement magnitudes. These sections were taken along the lines A-B (Panel 4N), and E-F (Panel 6N). Refer to Figure 12 for the position of these lines. The results are plotted in Figures 16 and 17 for Panels 4N and 6N respectively. The strong shear deformation (Section A-B) caused by the Merensky pillar punching into Panel 4N can be observed.

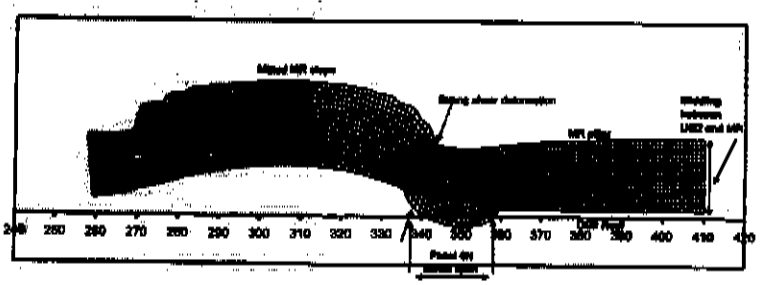

Figure 16 Plot showing the deformation of the middling between the Merensky and UG2 reef along Section A-B in Figure 12 (The values along the x-axis correspond to the values along the x-axis of Figure 12)

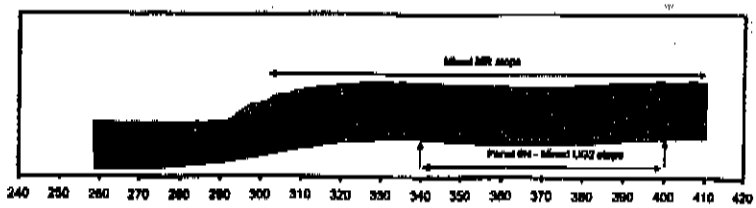

Figure 17 Plot showing the deformation of the middling between the Merensky and UG2 reef along Section E-F (Figure 12)

A key mechanism contributing to the observed inelastic closure is the prominent shear failure observed along the abutment next to the centre gully. This failure mode was investigated by simulating a plane-strain section normal to the reef plane (taken along Section 1-2 in Figure 12). A failure plane was introduced along the abutment between the edge of the Merensky and the UG2 stope horizons.

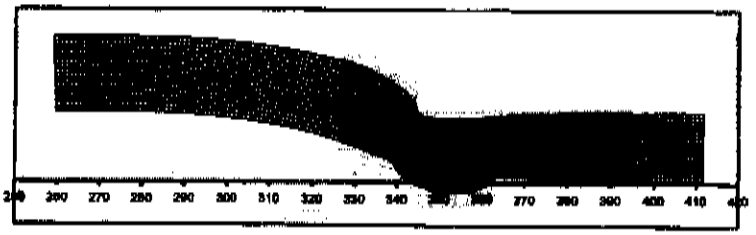

Figure 18 Plot showing the deformation of the middling between the Merensky and UG2 reefs for the 2D simulation. Note in this case the good agreement to the deformation determined for the 3D simulation (Figure 16)

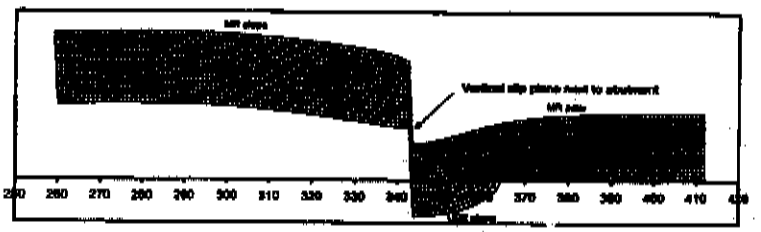

Figure 19 Plot showing the deformation of the middling between the Merensky and UG2 reef after the introduction of a vertical slip plane. This slip mechanism substantially increases the closure and ride deformations that arise in the stope

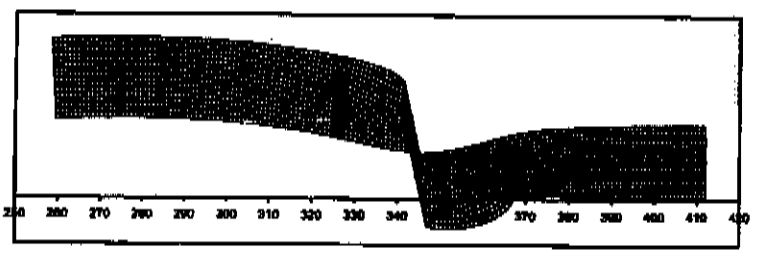

Figure 20 Plot showing the deformation of the middling between the Merensky and UG2 reef for an inclined slip plane

The simulated closure and ride for these simulations are given in Figures 21 and 22. Note that the introduction of the slip plane increases the closure significantly compared to that for the 3D simulation without the slip plane (Figure 14).

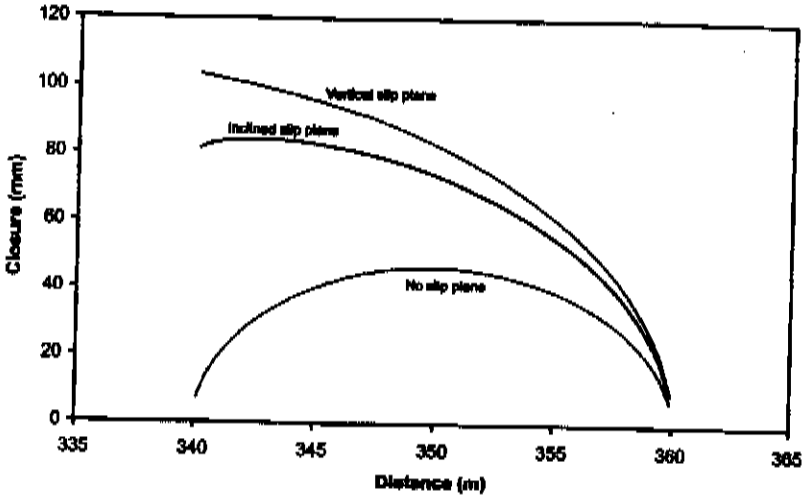

Figure 21 Closure in the panel for vertical and inclined slip planes. Note how the amount of closure increases when the slip plane is introduced

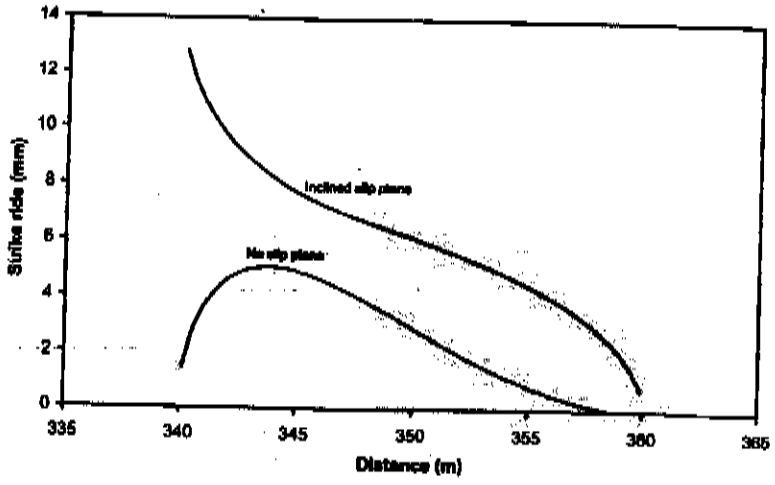

Figure 22 Ride in the panel with and without a slip plane

5 Conclusions

The paper describes the practical application of a new mine layout analysis computer code (TEXAN). This program was designed to solve typical multi-reef platinum mine layout problems encountered in the Bushveld Complex in South Africa at shallow depths. The program has a flexible computational structure to allow the efficient solution of problems that may include a large number of small, irregular pillars.

A particular investigation of the deformation mechanisms leading to large closure and strike ride components observed in a panel situated below a remnant is reported. Similar to the underground measurements, the elastic modelling indicated a noticeable ride component. The simulated values are much smaller than the observed values as the inelastic movements are not simulated explicitly. The sense of the ride is in agreement with that measured underground, namely the hangingwall moving relative to the footwall in the direction of the centre gully.

The mechanism of deformation was illustrated by computing off-reef displacement deformations to generate a distorted mesh plot of the region between the UG2 and Merensky reef planes. This plot illustrates how the edge of the overlying Merensky remnant punches into the UG2 stope below and causes strong shear deformation between the edge of the remnant and the abutment of the UG2 raise below. This mechanism appears to be the cause of the observed underground closure and ride movements.

The work described in this paper has shown that numerical modelling can play an important role in assessing appropriate mining strategies in a multiple reef environment. The analysis may be used to highlight areas where the stress levels are such that mining on the UG2 reef horizon will be impossible and superimposed pillars of unmined ground will have to be left.

References

Akermann, K., Altoumyan, P. and Van den Berg, T. (2003) Production of a stiff rockbolt and hanging wall control management system at a platinum mine in South Africa, In: M. Handley and D. Stacey (eds.) Proceedings of the 10th ISRM Congress, Johannesburg, pp. 11–17.

Day, A.P. and Godden, S.J. (2000) Design of panel pillars on Lonmin Platinum's Mines, Proceedings SANIRE 2000 Symposium, 2000.

Hartman, W. (2000) The application of the Q tunnelling quality index to rock mass assessment at Impala Platinum Mine. Proceedings SANIRE 2000 Symposium.

Joughin, W.C., Swart, A.H. and Wesseloo, J. (2000) Risk based chromitite pillar design – non-linear modelling, Proceedings SANIRE 2000 Symposium.

Malan, D.F., Napier, J.A.L and Janse van Rensburg, A.L. (2007) Stope deformation measurements as a diagnostic measure of rock behaviour: A decade of research, J. S. Afr. Inst. Min. Metall., Vol. 107, pp. 743–765.

Napier, J.A.L. and Malan, D.F. (2007) The computational analysis of shallow depth tabular mining problems, J. S. Afr. Inst Min Metall., Vol. 107, November 2007, pp. 725–742.

Napier, J.A.L. and Stephansen, S.J. (1987) Analysis of Deep-level Mine Design Problems Using the MINSIM-D Boundary Element Program, In: APCOM 87. Proceedings of the Twentieth International Symposium on the Applications of Computers and Mathematics in the Mineral Industries. Vol. 1: Mining, Johannesburg, SAIMM, pp. 3–19.

Ortlepp, W.D. and Nicoll, A. (1964) The elastic analysis of observed strata movement by means of an electrical analogue. J. S. Afr. Inst. Min. Metall. 65(4), pp. 214–235.

Roberts, D.P., Canbulat, I and Jack, B.W. (2002) Numerical modelling of pillar systems and investigation of controlling parameters. Proceedings SANIRE 2002 Symposium.

Ryder, J.A. and Jager, T. (2002) A textbook on rock mechanics for tabular hard rock mines. SIMRAC.

Ryder, J.A., De Maar, W. and Ozbay, M.U. (1997) A methodology for estimating the strength of hard rock support pillars, Gurtunca, R.G. and Hagan, T.O. Proc. SARES 1997, Johannesburg, pp. 435–439.

Salamon, M.D.G. (1964) Elastic analysis of displacements and stresses induced by the mining of seam or reef deposits - Part II: Practical methods of determining displacement, strain and stress components from a given mining geometry. J. S. Afr. Inst. Min. Metall., Vol. 64, pp. 197–218.

Watson, B.P. and Noble, K.R. (1997) Comparison between geotechnical areas on the Bushveld complex platinum mines, to identify critical spans and suitable in-panel support. R.G. Gurtunca and T.O. Hagan (editors), Proc. SARES 1997, Johannesburg, pp. 440–451.

Watson, B.P. and Roberts, D. (1999) A new approach to designing safe panel spans on the Merensky Reef. T.O. Hagan (editor) Proc. SARES99, Johannesburg, pp. 324–330.

Wesseloo, J. and Swart, A.H. (2000) Risk based chromitite pillar design – application of locally empirically derived pillar formula, Proceedings SANIRE 2000 Symposium.